# Upper-Tropospheric Synoptic-Scale Waves. Part I: Maintenance as Eady Normal Modes

CHANTAL RIVEST* AND CHRISTOPHER A. DAVIS**

*Center for Meteorology and Physical Oceanography, Massachusetts Institute of Technology, Cambridge, Massachusetts*

BRIAN F. FARRELL

*Harvard University, Department of Earth and Planetary Sciences, Cambridge, Massachusetts*

(Manuscript received 7 October 1991, in final form 20 February 1992)

ABSTRACT

Upper-tropospheric waves are important in midlatitude synoptic-scale dynamics. Their life duration is typically longer than time scales for disruption by the ambient shear and they often induce surface cyclogenesis. In this paper a dynamical model is proposed for the maintenance of these upper-level waves based on the upper-level Eady normal modes.

An analytical model of waves is developed on Eady basic states that have uniform tropospheric and stratospheric potential vorticity. While the standard Eady basic state represents the limiting case of infinite stratospheric static stability, it is found that the standard Eady normal-mode characteristics hold in the presence of realistic tropopause and stratosphere. In particular, the basic states studied support upper-level normal modes of synoptic scale, which are also nonlinear solutions of the quasigeostrophic equations.

It was demonstrated earlier that the upper-level modal solutions do not exist in the presence of even infinitesimal tropospheric gradients of potential vorticity. However, it is shown here that the limit of the Eady neutral mode is approached smoothly by solutions that decay even more slowly as the gradients of potential vorticity vanish.

## 1. Introduction

Upper-tropospheric waves of synoptic scale are important entities in midlatitude dynamics. They are ubiquitous and often induce surface cyclogenesis, a mode of development known as "type B," in contrast to "type A," where no upper-level predecessor is supposed to play an active role (cf. Peterssen and Smebye 1971). In a recent study of upper-tropospheric waves in the region of the jet stream, Sanders (1988) finds an average life duration of 12 days, characteristic eastward phase speed of 15 m $s^{-1}$, and wavelength of 2500 km. In this paper we propose a simple dynamical model for the maintenance of these upper-tropospheric waves: the upper-level Eady normal modes. These modes share many characteristics with observed midlatitude upper-level synoptic-scale waves and provide a simple model for their dynamics, as waves supported by the large latitudinal gradients of potential vorticity at the tropopause in the jet region.

Most previous studies of waves of synoptic scale in midlatitudes have dealt with the problem of their origin. There were the seminal papers of Eady (1949) and Charney (1947) that proposed the paradigm of linear waves embedded in an unstable basic state to explain cyclogenesis at the synoptic scale. Then Simmons and Hoskins (1976) extended the linear study to realistic basic states on the sphere, and furthermore examined the subsequent nonlinear evolution of the waves (Simmons and Hoskins 1978). Their simulations show first a linear development of a Charney-like wave with zonal wavelength of about 4000 km and with maximum amplitude at the surface, followed by an intensification at upper levels, and finally a barotropic decay with the formation of strong and narrow jets. More recently Thorncroft and Hoskins (1990) studied with a finer resolution the nonlinear evolution of initially linearly unstable waves. They found that, after the larger-scale cyclogenesis, troughs with wavelengths of about 1000 to 2000 km at upper levels can interact nonmodally with fronts at lower levels to produce strong cyclogenesis. This behavior is reminiscent of the cyclogenesis classified "type B" by Peterssen and Smebye (1971) and studied in the context of simplified models in Farrell (1984) and Rotunno and Fantini (1989).

Recently, Snyder and Lindzen (1988) have sought

* Present affiliation: Division de Recherche en Prévision Numérique, Atmospheric Environment Service, Canada.

** Present affiliation: National Center for Atmospheric Research.

*Corresponding author address:* Dr. Chantal Rivest, Atmospheric Environment Service, Division de Recherche en Prévision Numérique, 2121 Route Transcanadienne, Dorval, H9P 1J3 PQ Canada.

to explain the intensification at upper levels in terms of linear waves in evolving unstable basic states. They designed basic states with wind-shear increasing from the surface to the middle of the troposphere, relating them to basic states that are partially equilibrated by the wave. In the presence of boundary-layer friction linearly unstable modes with greatest amplitude in the interior of the flow are found. Whitaker and Barcilon (1992) addressed more directly the problem of the origin of upper-level waves as observed by Sanders (1988). These authors argue that the preferred regions for genesis, northwesterly flow over continents (Sanders 1988), are characterized by low-level baroclinicity and large surface roughness. They examine basic states with weak low-level baroclinicity, boundary-layer friction, and a tropopause defined by a larger static stability in the stratosphere, and they find linear unstable modes with maximum amplitude in the upper troposphere. Their work then explains the origin of upper-level waves in terms of the linear unstable waves of particular basic states.

In this paper we address the problem of the maintenance of the upper-level waves; a subsequent paper will be concerned at least partly with the problem of their origin. There were some partial answers in previous works where the problem was not addressed directly. In linear baroclinic instability theory, growth at upper levels seems to be favored in basic-state flow with weak low-level baroclinicity, boundary-layer friction, and a tropopause. In the nonlinear simulations, upper-level waves are characteristic of flows where the waves are past their linear stage of growth.

We study here waves on Eady basic states where the rigid lid is replaced by a finite, rather than infinite, jump in static stability: a flexible tropopause. In general our normal-mode solutions have the same qualitative character as those of the standard Eady basic state, and our results are consistent with the analysis of Muller (1991). Even if the flexible tropopause problem is mentioned in Eady (1949) and Gill (1983), it is not widely recognized that the Eady normal-mode characteristics hold not only for an unrealistic rigid lid but also for a realistic tropopause. Our presentation includes a discussion of the upper-level normal modes, which are nonlinear solutions of the quasigeostrophic equations. We show here with an analytical calculation and in a subsequent paper with linear simulations that these waves have counterparts in the linear Green model with positive interior gradients of potential vorticity, demonstrating that the disappearance of the upper-level modal solutions is not a singular limit.

In section 2 we formulate the problem mathematically; we present in section 3 the normal modes of an Eady basic state with a realistic tropopause; section 4 shows with an approximate calculation what happens to the upper-level normal modes in the presence of meridional gradients of potential vorticity, and in section 5 we discuss the overall significance of our study.

## 2. Mathematical formulation

### a. *Quasigeostrophic dynamics in a basic-state flow*

We choose the quasigeostrophic (QG) set of equations in their Boussinesq limit with uniform density to model the dynamics of upper-level synoptic-scale waves (Pedlosky 1979).

Consider perturbations $[q, \psi, u, v, w, \theta](x, y, z, t)$ in a basic-state flow $[Q, \Psi, U, \Theta](y, z)$, where $Q + q$ is the total QG pseudo-potential vorticity (QPV), $\Psi + \psi$ the geostrophic streamfunction, $U + u$ the zonal geostrophic wind, $v$ the meridional geostrophic wind, $w$ the vertical velocity, $\Theta + \theta$ the potential temperature, and where $(x, y, z, t)$ are the zonal, meridional, vertical, and time coordinates. The nondimensional equations for the basic state are

$$Q_y = \beta - \left[\frac{\partial^2}{\partial y^2} + \frac{\partial}{\partial z}\left(\frac{1}{N^2}\frac{\partial}{\partial z}\right)\right]U, \tag{1}$$

$$U = -\frac{\partial \Psi}{\partial y}, \tag{2}$$

$$\Theta = \frac{\partial \Psi}{\partial z}; \tag{3}$$

and for the perturbation fields:

$$\left[\frac{\partial}{\partial t} + U\frac{\partial}{\partial x} + J(\psi, )\right]q = -Q_y\frac{\partial \psi}{\partial x}, \tag{4}$$

$$\left[\frac{\partial}{\partial t} + U\frac{\partial}{\partial x} + J(\psi, )\right]\theta = -N^2 w - \Theta_y\frac{\partial \psi}{\partial x}, \tag{5}$$

where

$$q = \left[\nabla_H^2 + \frac{\partial}{\partial z}\left(\frac{1}{N^2}\frac{\partial}{\partial z}\right)\right]\psi, \tag{6}$$

$$u = -\frac{\partial \psi}{\partial y}, \quad v = \frac{\partial \psi}{\partial x}, \quad \theta = \frac{\partial \psi}{\partial z}, \tag{7}$$

$$J(A, B) \equiv A_x B_y - A_y B_x,$$

$$\nabla_H^2 \equiv \frac{\partial^2}{\partial x^2} + \frac{\partial^2}{\partial y^2};$$

$N^2(z)$ is the reference static stability profile, and $\beta$ is the latitudinal gradient of planetary vorticity.

These equations are completed by boundary conditions in the vertical and horizontal directions. At the lower boundary, the boundary condition on vertical velocity is chosen of the form:

$$w = \xi_l \nabla_H^2(\Psi + \psi), \tag{8}$$

where $\xi_l$ is a boundary-layer parameter.

Having chosen a vertical scale, $H$, the horizontal scale is the associated Rossby radius, $L \equiv N_0 H / f_0$. We also choose a velocity scale, $U_0$, a reference static stability $N_0$, potential temperature $\theta_0$, and density $\rho_0$, and an average planetary vorticity, $f_0$. It is then possible to

recover the dimensional variables and parameters (that are primed):

$$(x', y', z') = L\left(x, y, \frac{H}{L} z\right), \quad t' = \frac{L}{U_0} t,$$

$$N' = N_0 N, \quad \rho' = \rho_0 \rho,$$

$$(Q', q') = \mathrm{Ro} f_0 (Q, q), \quad (\Psi', \psi') = U_0 L (\Psi, \psi),$$

$$(U', u', v') = U_0 (U, u, v),$$

$$(\Theta', \theta') = \theta_0 \frac{f_0 L U_0}{gH} (\Theta, \theta),$$

$$w' = \mathrm{Ro} \frac{H}{L} U_0 w, \quad \beta' = \frac{\beta U_0}{L^2}, \tag{9}$$

where Ro is the Rossby number, $\mathrm{Ro} \equiv U_0/Lf_0$, and the boundary-layer parameter, $\xi_l$, is related to the eddy viscosity, $\nu$, as follows:

$$\xi_l = \frac{N_0}{U_0} \left(\frac{\nu}{2f_0}\right)^{1/2}. \tag{10}$$

*b. Normal modes in a zonal channel*

We consider normal models confined in a zonal channel and basic-state winds without meridional dependency. Such basic-state flows lead to a mathematical problem for the perturbation fields that is separable in $y$ and $z$. Actual studies of unstable waves on basic-state winds with meridional dependency have shown remarkable similarities with studies of artificially confined unstable waves (Simmons and Hoskins 1976; Ioannou and Lindzen 1986; Lin and Pierrehumbert 1988; Valdes and Hoskins 1988). The presence of barotropic shear usually acts to confine the perturbation in the jet axis, and to slightly reduce the instability.

From (1), (2), and (3), the basic-state equations are:

$$Q_y = \beta - \frac{d}{dz}\left(\frac{1}{N^2}\frac{dU}{dz}\right) \tag{11}$$

$$\Psi = -U(z) y, \tag{12}$$

$$\Theta = \frac{\partial \Psi}{\partial z}. \tag{13}$$

For perturbation fields of the form,

$$[q, \psi, v, w, \theta](x, y, z, t) = \mathrm{Re}([\hat{q}, \hat{\psi}, \hat{v}, \hat{w}, \hat{\theta}](z) e^{ik(x-ct)}) \sin ly, \tag{14}$$

$$u(x, y, z, t) = \mathrm{Re}(\hat{u}(z) e^{ik(x-ct)}) \cos ly, \tag{15}$$

where $l = \pi/L_y$, $k = 2\pi/L_x$, $L_y$ is the channel width, $L_x$ the zonal wavelength, and $c$ is a complex eigenvalue, $c = c_r + ic_i$ with $c_r$ being the phase speed and $kc_i$ the growth rate, the linear equations can be expressed as an eigenvalue problem for $\hat{\psi}$ and $c$ [from (4), (5), (6), (7)]:

$$(U - c)\left[\frac{d^2}{dz^2} - \frac{1}{N^2}\frac{dN^2}{dz}\frac{d}{dz} - N^2K^2\right]\hat{\psi} + N^2 Q_y \hat{\psi} = 0, \tag{16}$$

with $(U - c)\frac{d\hat{\psi}}{dz} + \Theta_y \hat{\psi} + i\frac{K^2}{k}\xi_l N^2 \hat{\psi} = 0$

$$\text{at} \quad z = 0, \tag{17}$$

$$\hat{\psi} \text{ bounded as } z \to \infty, \tag{18}$$

where $K^2 = k^2 + l^2$ is the total wavenumber.

From equations (5) to (7), the normal-mode solutions for the other perturbation fields are:

$$\hat{q} = -\frac{Q_y}{U - c}\hat{\psi}, \tag{19}$$

$$\hat{u} = -l\hat{\psi}, \quad \hat{v} = ik\hat{\psi}, \quad \hat{\theta} = \frac{\partial \hat{\psi}}{\partial z}, \tag{20}$$

$$\hat{w} = -\frac{ik}{N^2}\left[\Theta_y \hat{\psi} + (U - c)\frac{d\hat{\psi}}{dz}\right]. \tag{21}$$

There exist many theorems concerning the properties of normal-mode solutions, among which the Charney–Stern theorem is probably the best known (cf. Charney and Stern 1962). It states that a necessary condition for instability in the inviscid limit is that the meridional QPV gradient with appropriate contributions from the boundaries,

$$Q_y + \frac{\Theta_y}{N^2}(\delta(z_l) - \delta(z_u)),$$

changes sign over the domain.

*c. Basic states*

Let us assume no meridional gradient of planetary vorticity, $\beta = 0$. In each region we suppose uniform QPV and it follows from (11) that

$$\frac{d}{dz}\left(\frac{U_{iz}}{N^2}\right) = 0, \quad \text{for} \quad i = 1, 2, \tag{22}$$

where the subscript 1, 2 refers respectively to the troposphere and the stratosphere.

In the stratosphere we set constant zonal wind and stability,

$$U_2 = \text{const}, \quad N_2^2 = \text{const}, \quad \text{for } z > 1.$$

In the troposphere we set

$$U_1(z) = z, \quad N_1^2(z) = N_1^2 = 1 \quad \text{for } z < 1, \tag{23}$$

so that the constraint of uniform QPV is respected. Figure 1 displays vertical profiles of $U(z)$ and $N^2(z)$.

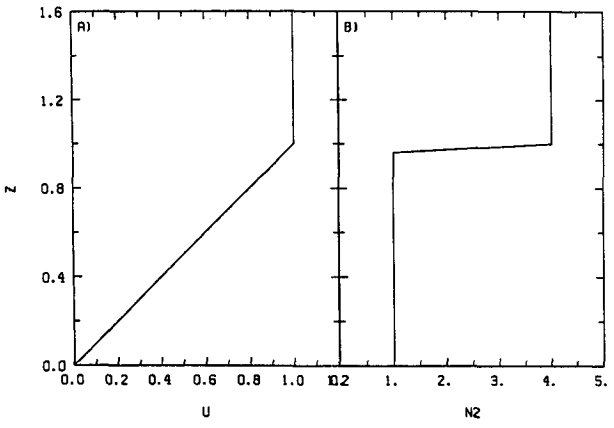


FIG. 1. The vertical profiles of basic state (a) wind $U(z)$, and (b) static stability $N^2(z)$, with $N_2^2 = 4$, for the Eady basic state with a flexible tropopause.

At the tropopause we can write from (11):

$$\int_{1-}^{1+} Q_y dz = -\frac{U_z}{N^2}\bigg|_{1-}^{1+} = \frac{U_{1z}(1)}{N_1^2(1)}$$

and hence:

$$Q_y = \frac{U_{1z}}{N_1^2}\,\delta(z-1) = -\frac{\Theta_{1y}}{N_1^2}\,\delta(z-1).$$

Following Bretherton (1966), we have at the ground:

$$Q_y = -\frac{U_{1z}}{N_1^2}\,\delta(z) = \frac{\Theta_{1y}}{N_1^2}\,\delta(z).$$

When the shear is positive in the troposphere, the $Q_y$ distribution of our generalized basic states is identical to that of the Eady one with sheets of positive and negative infinite $Q_y$ at the tropopause and ground. The necessary condition for instability stated in the Charney–Stern theorem is fulfilled. We can calculate the eddy QPV arising from the boundaries from (19):

$$\hat{q}(0) = -\frac{\Theta_{1y}}{N_1^2}\frac{\hat{\psi}}{(U-c)}\,\delta(z),$$

$$\hat{q}(1) = \frac{\Theta_{1y}}{N_1^2}\frac{\hat{\psi}}{(U-c)}\,\delta(z-1).$$

Since $c$ generally has a value typical of interior tropospheric wind, at the boundaries, positive (negative) $\hat{q}$ are collocated with negative (positive) $\hat{\psi}$.

It is possible to calculate the height variation of the tropopause with latitude. Let us consider the tropopause as a frontal interface where winds and temperatures are continuous but where their gradients are not. The slope of the frontal surface must then satisfy (Palmen and Newton 1969):

$$\left(\frac{dz}{dy}\right) \equiv -\mathrm{Ros} = -\mathrm{Ro}\,\frac{U_{1z}}{(N_2^2 - N_1^2)}, \quad \text{at} \quad z = 1. \quad (24)$$

The decrease of the tropopause height with latitude corresponds to a correction of the order of the Rossby number. In the limit of infinite stratospheric stability, $N_2^2 \to \infty$, the slope vanishes. Figure 2 shows the meridional distribution of isentropes for the basic state illustrated in Fig. 1.

*d. Perturbation equations*

In each region the equation for the eddy streamfunction follows from (16):

$$\left[\frac{d^2}{dz^2} - N_1^2K^2\right]\hat{\psi}_1 = 0, \quad (25)$$

$$\left[\frac{d^2}{dz^2} - N_2^2K^2\right]\hat{\psi}_2 = 0. \quad (26)$$

Therefore, from (17), we have as a boundary condition at the ground:

$$(U_1 - c)\frac{d\hat{\psi}_1}{dz} - U_{1z}\hat{\psi}_1 + i\frac{K^2}{k}\,\xi_l N_1^2\hat{\psi}_1 = 0 \quad \text{at} \quad z = 0, \quad (27)$$

while as an upper boundary condition we impose

$$\hat{\psi}_2 \text{ bounded as } z \to \infty. \quad (28)$$

These equations are completed by matching conditions at the tropopause. Let us introduce a new perturbation field,

$$h'(x', y', t') = \mathrm{Ro}Hh(x, y, t),$$

that represents the tropopause deformation associated with the wave. It is a correction of the order of the Rossby number to the basic-state tropopause height. We consider the tropopause as a material surface that separates low-tropospheric potential vorticity air from high-stratospheric potential vorticity air. The matching conditions are (Gill 1982):

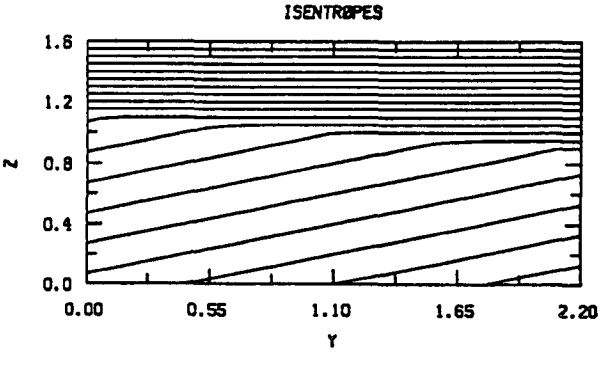


FIG. 2. Meridional–height cross section of basic state isentropes with $N_2^2 = 4$. The contour interval is 0.8.

$$\frac{D}{Dt}[z + \mathrm{Ro}(sy - h)] = 0,$$

$$\psi_1 = \psi_2, \quad \text{at} \quad z = 1 + \mathrm{Ro}(h - sy), \quad (29)$$

where $D/Dt$ is the Lagrangian derivative. After linearizing about the basic state, taking the limit $\mathrm{Ro} \to 0$, and considering normal-mode solutions, the matching conditions become:

$$\hat{\psi}_1(1) = \hat{\psi}_2(1), \quad (30)$$

$$\hat{w}_1(1) = \hat{w}_2(1), \quad (31)$$

or, from (21):

$$\frac{N_1^2}{N_2^2}(U_2 - c)\frac{d\hat{\psi}_2}{dz} = (U_1 - c)\frac{d\hat{\psi}_1}{dz} - U_{1z}\hat{\psi}_1, \quad \text{at} \quad z = 1.$$

*e. Perturbation tropopause motion*

From (29) it is possible to express $\hat{h}$ as

$$\hat{h} = \frac{(\hat{w} + s\hat{v})}{ik(U - c)} \quad \text{at} \quad z = 1, \quad (32)$$

or, using (21), as

$$\hat{h} = \frac{s}{(U - c)}\hat{\psi}_2 - \frac{1}{N_2^2}\frac{d\hat{\psi}_2}{dz}, \quad \text{at} \quad z = 1. \quad (33)$$

In the rigid-lid limit, $N_2^2 \to \infty$, the perturbation tropopause deformation vanishes since $\hat{w}(1) = s = 0$. For the waves considered in this paper, $U(1) - c > 0$ and the streamfunction decays with height in the stratosphere. Therefore, $\hat{h}$ and $\hat{\psi}_2$ are generally correlated, with cyclones (anticyclones) associated with low (high) tropopauses. When the wave is unstable, there is an added phase shift, and the tropopause perturbation is located upstream of the streamfunction perturbation. In the context of linear QG theory this deformation does not feed back on the wave characteristics.

*f. Solutions*

We introduce a class of analytical solutions to the system of equations (25), (26), (27), (28), (30), and (31). We have in the stratosphere, from (26) and (28):

$$\hat{\psi}_2(z) = A_2 \exp[-\alpha_2(z - 1)],$$

where

$$\alpha_2^2 = N_2^2K^2;$$

and in the troposphere [from (25)]:

$$\hat{\psi}_1(z) = [A_{1c}\cosh(\alpha_1 z) + A_{1s}\sinh(\alpha_1 z)],$$

where

$$\alpha_1^2 = N_1^2K^2.$$

Substituting these solutions into the matching and boundary conditions (30), (31), and (27) leads to a quadratic expression for $c$:

$$\mathcal{A}c^2 + \mathcal{B}c + \mathcal{C} = 0,$$

where:

$$\mathcal{A} \equiv \alpha_1 F_1$$

$$\mathcal{B} \equiv -\left[\alpha_1 F_1 - \alpha_1 C_1 + G_1\left(1 - i\frac{\xi_l\alpha_1^2}{k}\right)\right]$$

$$\mathcal{C} \equiv (G_1 - S_1)\left(1 - i\frac{\xi_l\alpha_1^2}{k}\right),$$

with

$$F_1 \equiv \alpha_1(S_1 + \sigma C_1),$$

$$G_1 \equiv \alpha_1(C_1 + \sigma S_1),$$

$$C_1 \equiv \cosh\alpha_1, \quad S_1 \equiv \sinh\alpha_1.$$

This expression for $c$ also determines $\hat{\psi}_1(z)$ through the boundary and matching conditions. The other perturbation fields can be calculated using the formulas (19), (20), and (21).

*g. Parameter values*

In this paper we are concerned with synoptic-scale motions in the region of the jet. We choose $f_0 = 10^{-4}\,\mathrm{s}^{-1}$, $g = 10\,\mathrm{m\,s}^{-2}$, $N_0 = 10^{-2}\,\mathrm{s}^{-2}$, $\beta' = 1.6 \times 10^{-11}\,\mathrm{m\,s}^{-1}$, and $H = 9$ km, roughly the tropopause height in the middle of the jet. This value of $H$ implies a Rossby radius, $L = 900$ km. We set $U_0 = \gamma_0 H$, where $\gamma_0$ is an average tropospheric shear so that fixing $\gamma_0 = 3\,\mathrm{m\,s}^{-1}/\mathrm{km}$ yields $U_0 = 27\,\mathrm{m\,s}^{-1}$. For these values the nondimensional beta and the Rossby number are $\beta = 0.5$ and $\mathrm{Ro} = 0.3$. Table 1 displays the correspondence between dimensional and nondimensional variables.

We also consider a channel with $l = 1.4$, that is, of nondimensional and dimensional widths $L_y = 2.2$ and $L_y' = 2000$ km (see Table 1). This implies a tropospheric potential temperature change across the channel of $\Delta\Theta = \Theta_y L_y = 2.2$ (dimensionally $\Delta\Theta' = 18$ K). The basic-state zonal wind maximizes at the tropopause where it is unity ($27\,\mathrm{m\,s}^{-1}$). We fix the upper-tropo-

TABLE 1. Dimensional and nondimensional variables; $Z'$ is the height at a pressure surface typical of the tropopause, and $P'$ is the pressure at the ground.

| |
|---|
| $(x', y') = 900$ km $(x, y)$ |
| $(z') = 9$ km $(z)$ |
| $(t') = 0.39$ day $(t)$ |
| $(Z'(z = 1)) = 24$ dm $(\psi)$ |
| $(P'(z = 0)) = 24$ hPa $(\psi)$ |
| $(U', u', v') = 27\,\mathrm{m\,s}^{-1}$ $(U, u, v)$ |
| $(\Theta', \theta') = 8.1$ K $(\Theta, \theta)$ |
| $(w') = 8.1\,\mathrm{cm\,s}^{-1}$ $(w)$ |

spheric stability to unity $N_1^2(1) = 1$ ($10^{-4}$ s$^{-2}$) while in most cases $N_2^2 = 4$. The boundary-layer parameter $\xi_l$ takes values typical of oceanic, flat landmass, and mountainous landmass terrains, $\xi_l = 0.04, 0.08, 0.12$, which corresponds to eddy viscosity, $\nu$, of 1, 5, and 20 m$^2$ s$^{-1}$, as discussed in Lin and Pierrehumbert (1988).

## 3. Normal-mode results

### a. *The inviscid edge wave solutions*

We discuss in this section the edge wave solutions that arise in the limit of small horizontal scales. Even if they strictly apply in that limit only, they are interesting because of their simplicity and because similar dynamics characterizes a wide range of scales.

In the limit of small horizontal length scales the vertical depth of the perturbation $\psi$ becomes much less than the tropopause height. Then, the perturbation $q$'s, necessarily confined at the ground and tropopause, do not "feel" each other via their associated circulation and we have two independent edge wave solutions, one at each boundary. Mathematically we take the limit

$$K^2 = k^2 + l^2 \gg 1.$$

Then, taking the additional inviscid limit, $\xi_l \to 0$, we get for the edge wave at the ground:

$$\hat{\psi}_1(z) = \exp(-Kz), \quad c = \frac{U_{1z}(0)}{K}.$$

A comprehensive discussion of this solution is given in Gill (1982).

It is an interesting case of a modal wave that remains neutral in the presence of available potential energy in the basic-state flow. The phase lines of eddy fields are vertical; therefore, the wave does not transport heat meridionally and does not grow. It is called a boundary or edge wave since it decays away from the ground. The wave translates with speed $c$, that is, with the basic-state wind one Rossby height (or an $e$-folding scale $H_R = 1/K$) above the surface. Low (high) pressure perturbations are collocated with warm (cold) temperature perturbations, and the phase of the vertical velocity field is advanced 90° ahead of that of the streamfunction field with upward (downward) motions leading low (high) pressure perturbations.

Taking the same limits as previously, we get an interfacial edge wave solution at the tropopause with

$$\hat{\psi}_1(z) = \exp K(z-1), \quad \hat{\psi}_2(z) = \exp - N_2K(z-1),$$

$$c = 1 - \frac{U_{1z}(1)}{K(1 + N_2^{-1})}.$$

From (33) and (24), it is possible to calculate the amplitude of the perturbation tropopause deviation:

$$|\hat{h}| = K\left(\frac{1}{N_2^2 - 1} + \frac{1}{N_2}\right).$$

As shown in Fig. 3, when the stability increases in the stratosphere, the phase speed and the amplitude of the tropopause motion decrease. At $k = 2.3$, $c = 0.75$ and $|\hat{h}| = 2.2$ for $N_2^2 = 4$. Using Table 1, these numbers correspond to a zonal wavelength of 2500 km, to a steering level located at 6.7 km with basic-state wind speed of 20 m s$^{-1}$, and to a tropopause deviation of 1.2 km for a perturbation height of 5 dm.

Figure 4 displays characteristics of the wave solution at $k = 2.3$. They are very similar to those of the lower-level edge wave. Above the tropopause the relative phase and vertical profiles of most perturbation fields such as streamfunction, temperature, and vertical velocity are similar, and low (high) pressure perturbations have associated warm (cold) temperature perturbations. Below the tropopause the relative phase of the perturbation potential temperature is different, with cold (warm) air embedded in cyclones (anticyclones). In Fig. 4 the vertical velocity does not vanish at $z = 0$ since in the limit taken at the beginning of this section, the ground and the tropopause are considered to be much farther apart than the depth of the wave. For an upper-level wave of amplitude 0.2 at the tropopause (dimensionally 5 dm), the amplitude of the temperature perturbation is of 0.85 (7 K) in the stratosphere and of 0.55 (4.5 K) in the troposphere. The maximum

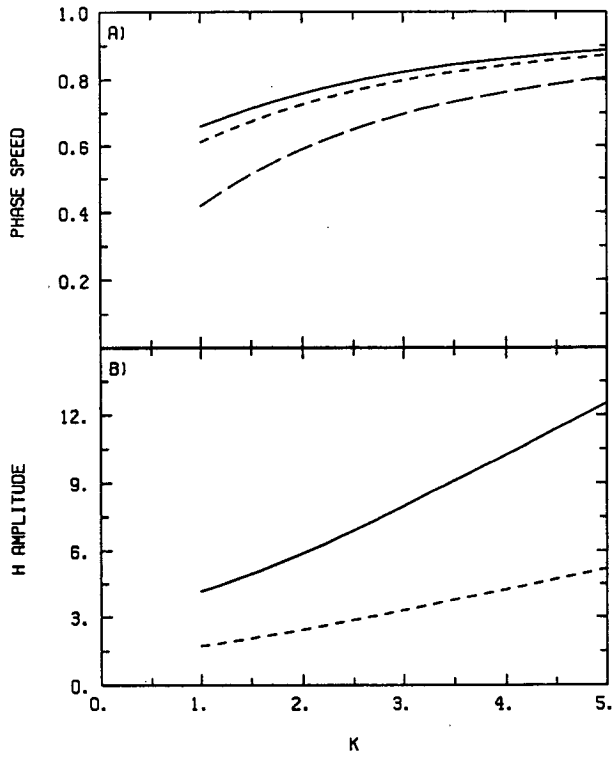


FIG. 3. (a) Phase speed $c$, and (b) tropopause motion amplitude $|\hat{h}|$ of the upper-level edge-wave solutions as a function of $k$ for different values of $N_2^2$ ($N_2^2 = 2$, solid line; $N_2^2 = 4$, short-dash line; $N_2^2 = \infty$, long-dash line). The streamfunction amplitude is fixed to unity at the tropopause.

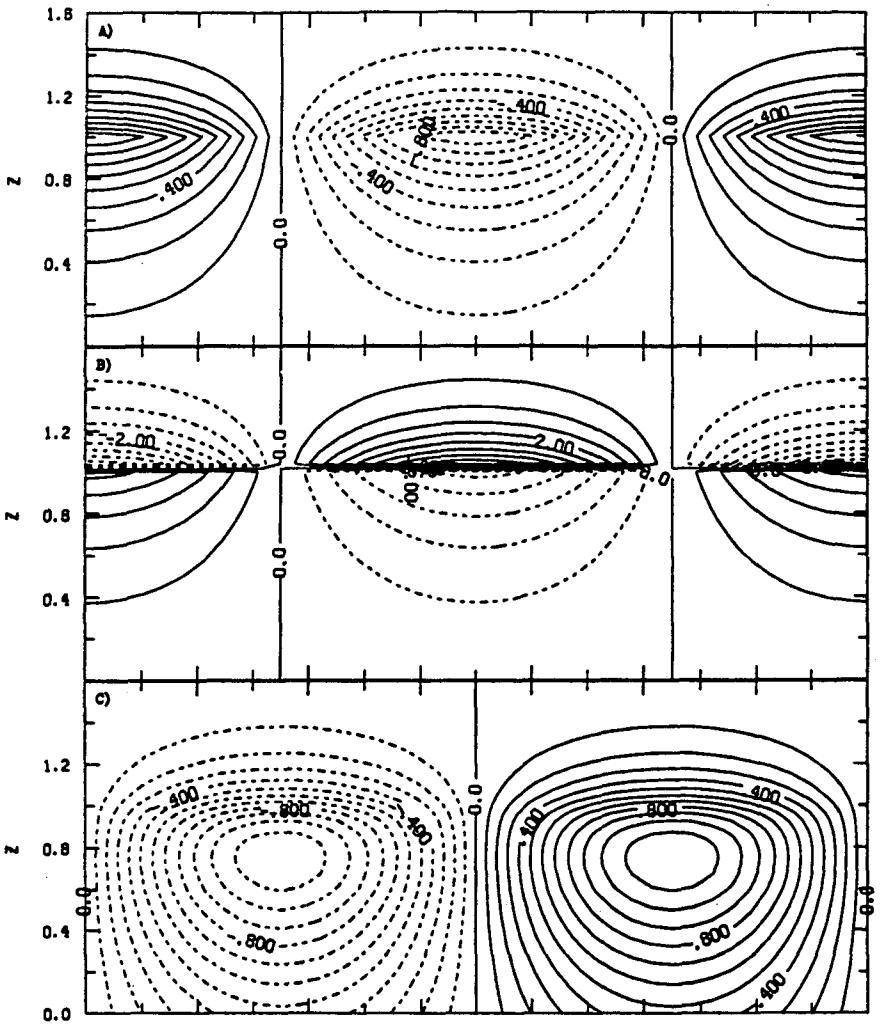


FIG. 4. Midchannel $x$–$z$ cross section of the upper-level edge wave at $k = 2.3$ with $N_2^2 = 4$: (a) streamfunction, (b) potential temperature, and (c) vertical velocity. The contour interval is 0.1 in (a), 0.5 in (b), and 0.1 in (c), and the streamfunction amplitude at the tropopause is fixed to unity.

meridional wind speed is then 0.46 (12 m s$^{-1}$) and the vertical wind speed attains 0.3 (2 cm s$^{-1}$).

Notice that at the tropopause the potential temperature perturbation is discontinuous. This peculiarity can be explained by looking at the vertical profiles of particle trajectories and of isentropes. For the upper-level edge-wave solution the vertical and meridional velocities are in phase; therefore, it is possible to write the particle trajectories in the $y$–$z$ plane as

$$\left(\frac{\delta z}{\delta y}\right) = \mathrm{Ro}\,\frac{w}{v},$$

and the isentropic slope is

$$\left(\frac{\delta z}{\delta y}\right)_\theta = -\mathrm{Ro}\,\frac{\Theta_y}{N^2}.$$

As shown in Fig. 5, the slope of the basic-state isentropes changes abruptly at the tropopause. Following the trajectories in the figure, particles above the tropopause, previously warmer than their surroundings, find themselves colder than their surroundings. Another way to explain the discontinuous temperature profiles is to examine the thermodynamic equation, (5). Above the tropopause the dominant process is adiabatic warming or cooling, whereas below it is advection of basic-state potential temperature.

### *b. The total inviscid solutions*

Let us now keep the interaction between the two boundary QPV perturbations that was absent in the previous section and look at the total inviscid solutions. At large enough scales the phase of perturbation fields is no longer vertical and the normal modes can release the available energy of the basic state.

Figures 6 to 8 display propagation and instability characteristics of the normal modes and the structure

of the most unstable modes for two different basic states. Using these figures, we can examine the effects of a realistic tropopause on the waves. The solid and small dash lines represent, respectively, the rigid-lid limit (the standard Eady basic state) and a realistic tropopause. As shown in Fig. 6a, which displays the growth rate ($\Omega = kc_i$), passage from a lid to a tropopause moves the normal-mode instability toward larger scales and decreases the maximum growth rate. The maximum growth rate is reduced by a factor of 1.4, from 0.2 to 0.14 (that correspond to $e$-folding times of 2.0 and 2.7 days), and moved from $k = 1.3$ to $k = 1$ ($L'_x = 4300$ and 5700 km). Also, the phase speeds of unstable modes and of neutral upper-level modes generally increase when the tropopause becomes more flexible (see Fig. 6b). The tropopause motion, which vanishes in the rigid-lid limit, is present with a realistic tropopause. As shown in Fig. 7b, for growing waves, the perturbation tropopause motion moves slightly upstream of the streamfunction. The structure of the most unstable mode is also altered by the addition of a realistic tropopause: the perturbation streamfunction is less developed at the upper level and the phase lines are more vertical, as can be seen from Figs. 8a and 8b.

Figure 9 displays characteristics of the upper-level normal mode at $k = 2.3$ for the basic state with the flexible tropopause. Let us remark that this normal mode is a nonlinear solution of the quasigeostrophic equations (4) and (5): the Jacobians vanish since the phase lines are vertical. It is interesting to compare Fig. 9 with Fig. 4, which represents the upper-level edge-wave solution at the same scale in the absence of the lower boundary. At upper levels most characteristics

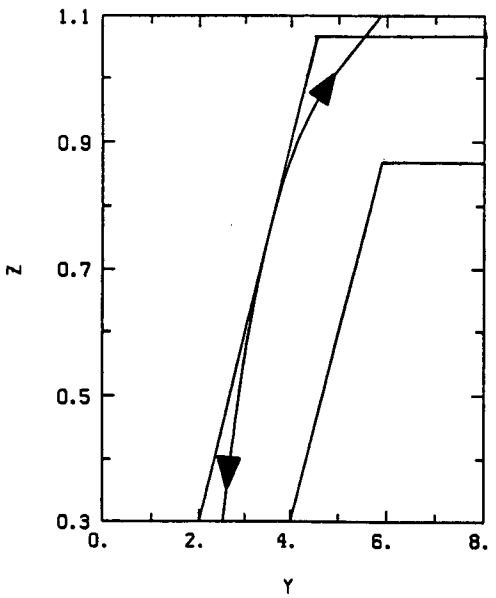


FIG. 5. Particle trajectory of the upper-level edge wave and basic-state isentropes in the $y$–$z$ plane at $k = 2.3$ with $N_2^2 = 4$. The line with the arrows represents the particle trajectory, while the two other lines are isentropes.

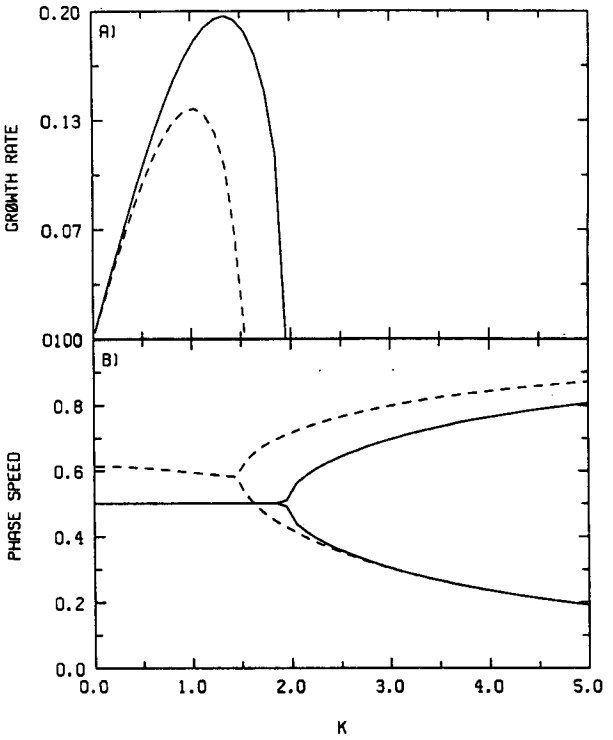


FIG. 6. (a) Growth rate $\Omega$ and (b) phase speed $c_r$ of inviscid solutions as a function of $k$ for two different basic states: the standard Eady basic state (solid line) and the basic state with $N_2^2 = 4$ (dash line).

of the two solutions, such as the amplitude and phase of different fields, are remarkably similar. The dynamics of the normal-mode solution at this scale are therefore expected to be very similar to that of the edge wave. However, the presence of the ground creates secondary extrema in the streamfunction field. As seen in Fig. 9a, the amplitude at the ground is about one-fourth of that at the tropopause. So, for a perturbation amplitude of 0.2 (5 dm) at the tropopause, a surface pressure perturbation of 1.5 hPa is expected.

### c. *The effects of boundary-layer friction*

We examine here the effect of friction at the lower boundary. This problem has been addressed in Williams and Robinson (1974) with results similar to ours, but lacking our emphasis on the upper-level normal modes that are destabilized by friction at the lower boundary. Figure 10 shows the growth and decay rates of normal modes for four values of the friction parameter $\xi_l$. The presence of friction reduces the instability at large scales, damps very strongly the lower-level wave solutions, and slightly destabilizes the upper-level wave solutions. For $\xi_l = 0.12$, a value typical of mountainous terrains, the growth rate of the upper-level wave is 0.005 at $k = 2.3$, which corresponds to an $e$-folding time of 80 days; for the lower-level wave, the decay rate is 0.33, which corresponds to an $e$-folding time of 1.2 days.

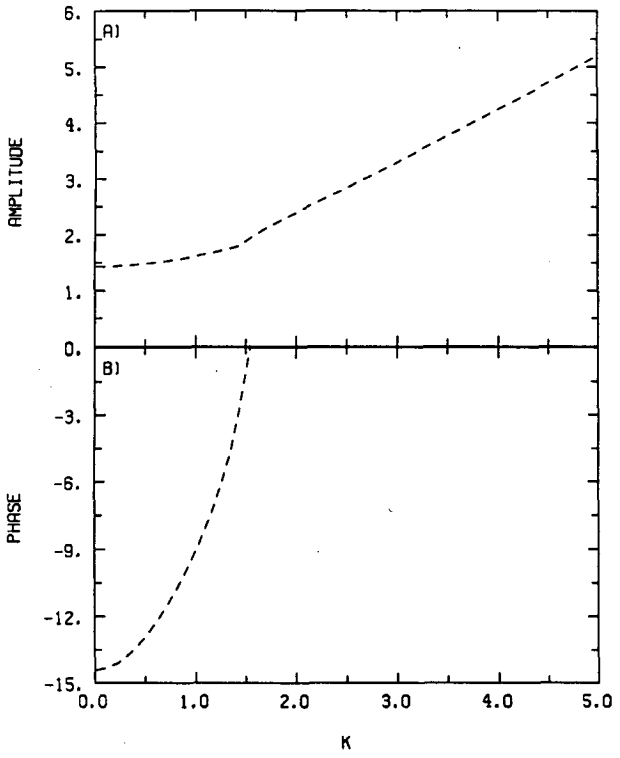


FIG. 7. The tropopause deviation $\hat{h}$ (a) amplitude and (b) phase of inviscid solutions as a function of $k$ for the two basic states represented as in Fig. 6.

Let us try to understand how the friction at the lower boundary acts on lower-level and upper-level waves. In the formulation presented in section 2a, frictions induces upward and downward motion in areas of low and high pressures, respectively. Within the QG system this creates adiabatic cooling and warming in low and high pressure areas so that the friction tends to destroy lower-level waves that have warm depressions, and slightly destabilized upper-level ones that have cold depressions. It is interesting to note that this destabilization of upper-level waves does not require a temperature gradient (or equivalent $Q_y$) at the ground.

Figure 11 displays characteristics of the upper-level wave solution at $k = 2.3$ for a friction parameter typical of a mountainous landmass. Comparing Figs. 3.12 and 3.9, we notice that the fields at upper levels are unchanged. At lower levels, there is an upshear tilt in the streamfunction field, while the temperature and vertical velocity fields show downstream tilt, indicating positive baroclinic energetics and extraction of the basic-state energy.

## 4. The effects of positive tropospheric gradients of potential vorticity

There is an argument against proposing the upper-level Eady normal modes as a conceptual model for atmospheric waves: these upper-level normal-mode solutions no longer exist in the presence of positive tropospheric gradients of potential vorticity (Green 1960). In this section we show with an analytic approximation what happens to them when such gradients are introduced: they slowly decay with time. In a subsequent paper we will report on their mathematical structure and also on how they can be excited in the presence of positive tropospheric QPV gradients.

For simplicity we consider here a basic state with constant shear, $U(z) = z$, and constant static stability, $N^2 = 1$. We assume a semi-infinite domain, $-\infty < z < z_u$, bounded by an inviscid rigid lid at $z_u = 1$. This assumption is reasonable because the results in section 3b show that the dynamics of the upper-level normal mode at $k = 2.3$ is very similar to those of the upper-level edge wave. From (11), the interior meridional QPV gradient reduces to the form: $Q_y = \beta$ and the contribution from the upper boundary is equivalent to a thin sheet of positive $Q_y$ (Bretherton 1966). From the Charney–Stern theorem, unstable modes cannot

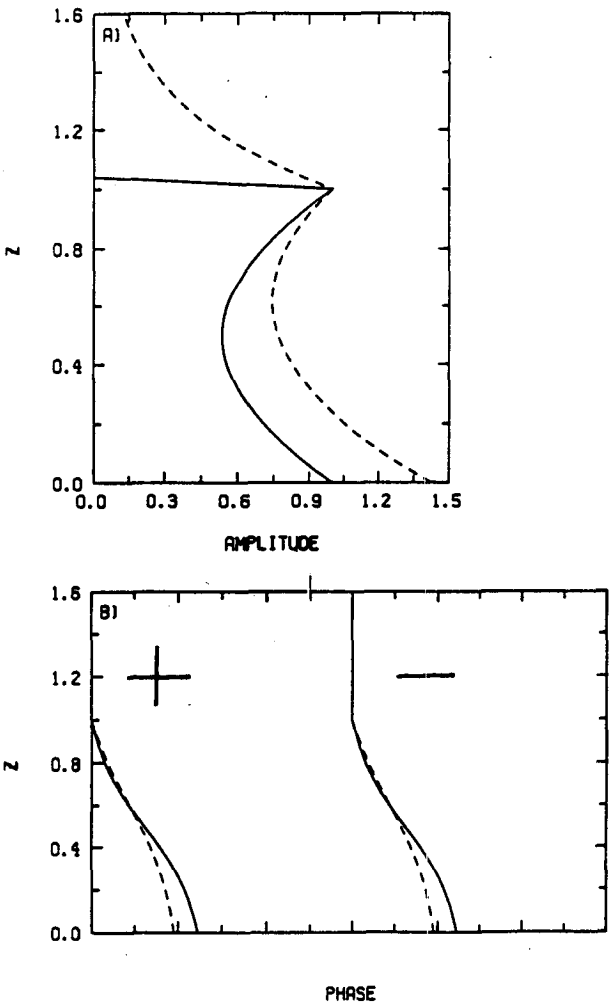


FIG. 8. The vertical profiles of streamfunction $\hat{\psi}$ (a) amplitude and (b) phase of inviscid solutions most unstable modes for the two basic states represented as in Fig. 6. The streamfunction at the tropopause is fixed to unity.

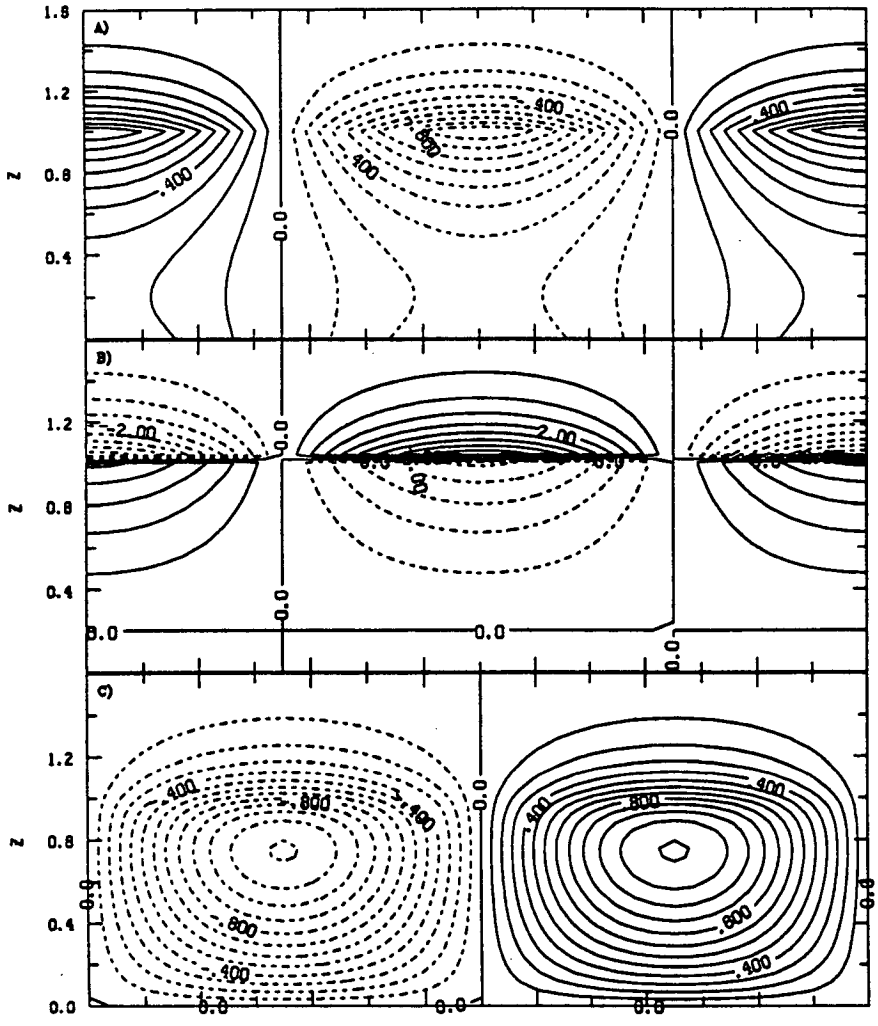


FIG. 9. Midchannel $x$–$z$ cross section of the inviscid upper-level normal mode at $k = 2.3$ with $N_2^2 = 4$: (a) streamfunction, (b) potential temperature, and (c) vertical velocity. The contour interval is 0.1 in (a), 0.5 in (b), and 0.1 in (c), and the streamfunction amplitude at the tropopause is fixed to unity.

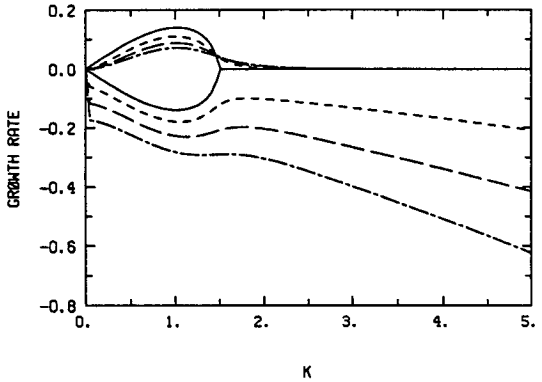


FIG. 10. Growth and decay rate ($kc_i$) of viscous solutions as a function of $k$ for the basic state with $N_2^2 = 4$ and for different values of $\eta_l$: $\eta_l = 0$, solid line; $\eta_l = 0.04$, small-dash line; $\eta_l = 0.08$, long-dash line; $\eta_l = 0.12$, small dash–long dash line.

exist in this system. Furthermore, the one-signedness of the $Q_y$ distribution also forbids the existence of neutral modes (Bretherton 1966).

Some integral relationships help to reveal the important aspects of the dynamics (Pedlosky 1979). First we can use the result that the meridional eddy flux of QPV has to be balanced by the meridional eddy flux of heat at the boundary:

$$(\overline{v\theta}|^{z=1} = \int_{-\infty}^{1} dz\overline{vq}, \tag{34}$$

where

$$\overline{(\ )} = \frac{1}{L_x}\int_0^{L_x} dx(\ ).$$

This relation allowed Bretherton (1966) to develop his argument for the nonexistence of neutral modes in ba-

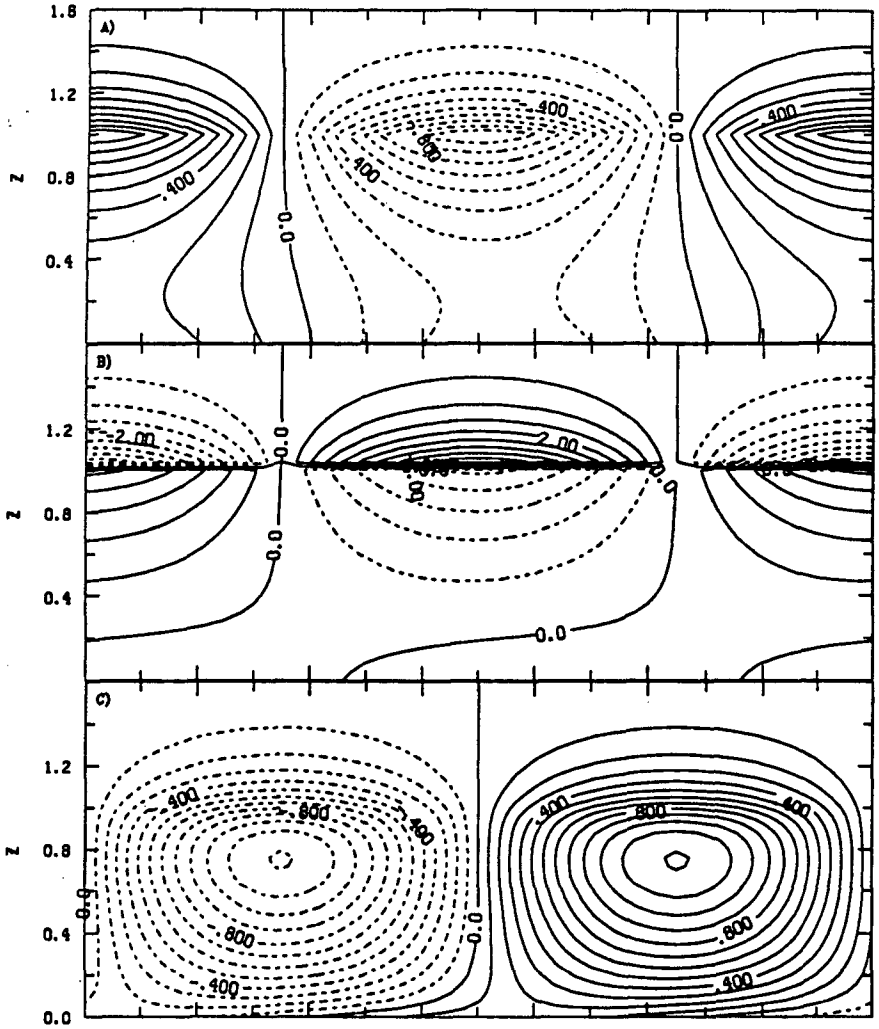


FIG. 11. Midchannel $x$–$z$ cross section of the viscous upper-level normal mode at $k = 2.3$ with $N_2^2 = 4$ and $\eta_I = 0.12$ : (a) streamfunction, (b) potential temperature, and (c) vertical velocity. The contour interval is 0.1 in (a), 0.5 in (b), and 0.1 in (c), and the streamfunction amplitude at the tropopause is fixed to unity.

sic states with one-signed $Q_y$. The lhs of (34) can be rewritten as

$$(\overline{v\theta}|^{z=1} = \frac{\partial}{\partial t}(\overline{\eta^2/2}|^{z=1}, \tag{35}$$

where $\eta$ represents the meridional displacement. In the case of neutral modes propagating with phase speed $c$, we can express the rhs of (34) as

$$\int_{-\infty}^{1} dz\overline{vq} = -\beta \int_{z_c-}^{z_c+} dz \frac{\partial}{\partial t}(\overline{\eta^2/2}),$$

$$= -\beta\pi k\left(\frac{\overline{\psi^2}}{U_z}\right|^{z=z_c}, \tag{36}$$

where $z_c$ is the height of the critical level, $U(z_c) = c$. To obtain (36) we took the physical limit of viscosity going to zero from positive values. Comparing (35) and (36) we see that if a neutral mode were to exist it would produce a QPV flux at its critical level that cannot be balanced for a neutral mode because the temperature flux at the boundary vanishes. This contradiction proves that neutral modes with interior critical layer cannot exist in a flow with nonzero $Q_y$.

Let us further approximate the streamfunction field as

$$\psi(z, t) \approx \hat{\psi}_E(z)e^{-\Lambda_n t}e^{ikc_E t},$$

where $\Lambda_n$ is the decay rate in the normal-mode limit, and $\hat{\psi}_E(z)$ and $c_E$ are, respectively, the streamfunction field and phase speed associated with the upper-level edge-wave solution in the limit of infinite stratospheric stability,

$$\hat{\psi}_E(z) = \exp[K(z-1)], \quad c_E = 1 - 1/K, \tag{37}$$

(see section 3a). Then, through (35), the lhs of (34) can be approximated as

$$(\overline{v\theta}|^{z-1} \approx -\frac{\Lambda_n}{2}\frac{(|\hat{\psi}_E|^2|^{z=1}}{(1-c_E)^2}\sin^2 ly$$

$$= -\frac{\Lambda_n}{2(1-c_E)^2}\sin^2 ly,$$

since $\hat{\eta} = \hat{\psi}/(U-c)$, while the rhs reduces from (36) to

$$\int_{-\infty}^{1} dz\overline{vq} \approx -\frac{\beta\pi k}{2e^2}\sin^2 ly.$$

These lead to a decay rate,

$$\Lambda_n \approx \frac{\beta\pi k}{e^2(k^2+l^2)}. \tag{38}$$

In a subsequent paper we will show that this result is a very good approximation to the decay rate observed in initial-value experiments. For values $\beta = 0.5$, $k = 2.3$, and $l = 1.4$, which correspond to zonal wavelength of 2500 km and channel width of 2000 km, the amplitude of the upper-level edge wave decays by an exponential factor in 15 time units, dimensionally 6 days. Moreover, this value of $\beta$ can be considered as an upper bound for tropospheric $Q_y$ since observations of tropospheric meridional gradients of Ertel potential vorticity along isentropes reveal these gradients to be very small (Hoskins et al. 1985).

## 5. Conclusions

We have proposed a simple dynamical model for the maintenance of midlatitude upper-level synoptic-scale waves based on analytical solution for waves on Eady basic states with realistic tropopause and stratosphere. We showed that the standard Eady normal-mode characteristics hold in the presence of these generalizations, and that this model supports at the synoptic-scale upper-level neutral normal modes, which share many characteristics with midlatitude upper-level synoptic-scale waves.

Moreover, we demonstrated with an approximate calculation that the upper-level normal modes are only slowly decaying in the presence of positive tropospheric gradients of potential vorticity, so that the result of Green (1960)—that no neutral upper-level normal modes exist in the presence of QPV gradients—is shown not to constitute an important physical objection to this theory for the maintenance of the upper-level waves. In a subsequent paper we will explain in more detail the mathematical structure of the upper-level waves in the presence of such gradients and we will also be concerned with the excitation of these waves.

In general the upper-level troughs followed by Sanders (1988) are wave packets that consist of a superposition of waves of different zonal wavenumbers. It is beyond the scope of this study to examine the localized nature of the short waves. In our opinion, to treat this problem correctly, one has to consider the full nonlinear dynamics existing at the tropopause in the jet region.

*Acknowledgments.* The authors wish to thank Kerry A. Emanuel and R. Alan Plumb for stimulating discussions. Isaac Held is to be thanked for his help in deriving the approximate decay rate in section 4. This work was supported by the National Science Foundation under Grant ATM-8513871. The first author acknowledges support from the "Fonds pour la formation de chercheurs et l'aide la recherche du Quebec" and from Zonta International. The first author also thanks Jean-Francois Geleyn for his hospitality at the French Weather Service.

## REFERENCES

Bretherton, F. P., 1966: Critical layer instability in baroclinic flows. *Quart. J. Roy. Meteor. Soc.*, **92**, 325–334.

Charney, J. G., 1947: The dynamics of long waves in a baroclinic westerly current. *J. Meteor.*, **4**, 135–162.

——, and M. E. Stern, 1962: On the stability of internal baroclinic jets in a rotating atmosphere. *J. Atmos. Sci.*, **19**, 159–172.

Eady, E. T., 1949: Long waves and cyclone waves. *Tellus*, **1**, 33–52.

Farrell, B., 1984: Modal and non-modal baroclinic waves. *J. Atmos. Sci.*, **41**, 668–673.

Gill, A. E., 1982: *Atmosphere-Ocean Dynamics.* Academic Press, 662 pp.

Green, J. S. A., 1960: A problem in baroclinic stability. *Quart. J. Roy. Meteor. Soc.*, **86**, 237–251.

Hoskins, B. J., M. E. McIntyre, and A. W. Robertson, 1985: On the use and significance of isentropic potential vorticity maps. *Quart. J. Roy. Meteor. Soc.*, **111**, 877–946.

Ioannou, P., and R. S. Lindzen, 1986: Baroclinic instability in the presence of barotropic jets. *J. Atmos. Sci.*, **43**, 2999–3014.

Lin, S. J., and R. T. Pierrehumbert, 1988: Does Ekman friction suppress baroclinic instability? *J. Atmos. Sci.*, **45**, 2920–2933.

Muller, J. C., 1991: Baroclinic instability in a two-layer, vertically semi-infinite domain. *Tellus*, **43A**, 275–284.

Palmen, E., and C. W. Newton, 1969: *Atmospheric Circulation Systems.* Academic Press, 603 pp.

Pedlosky, J., 1979: *Geophysical Fluid Dynamics.* Springer-Verlag, 624 pp.

Peterssen, S., and S. J. Smebye, 1971: On the development of extratropical cyclones. *Quart. J. Roy. Meteor. Soc.*, **97**, 457–482.

Rotunno, R., and M. Fantini, 1989: Peterssen's type B cyclogenesis in terms of discrete, neutral Eady modes. *J. Atmos. Sci.*, **46**, 3599–3604.

Sanders, F., 1988: Life history of mobile troughs in the upper westerlies. *Mon. Wea. Rev.*, **118**, 2629–2648.

Simmons, A. J., and B. J. Hoskins, 1976: Baroclinic instability on the sphere: Normal modes of the primitive and quasigeostrophic equations. *J. Atmos. Sci.*, **33**, 1454–1477.

——, and ——, 1978: The life cycles of some nonlinear baroclinic waves. *J. Atmos. Sci.*, **35**, 414–432.

Snyder, C., and R. S. Lindzen, 1988: Upper-level baroclinic instability. *J. Atmos. Sci.*, **45**, 2445–2459.

Thorncroft, C. D., and B. J. Hoskins, 1990: Frontal cyclogenesis. *J. Atmos. Sci.*, **47**, 2317–2336.

Valdes, P. J., and B. J. Hoskins, 1988: Baroclinic instability of the zonally averaged flow with boundary-layer damping. *J. Atmos. Sci.*, **45**, 1584–1593.

Whitaker, J. S., and A. Barcilon, 1992: Genesis of mobile troughs in the upper westerlies. *J. Atmos. Sci.*, **49**, 2111–2121.

Williams, G. P., and J. B. Robinson, 1974: Generalized Eady waves with Ekman pumping. *J. Atmos. Sci.*, **31**, 1768–1776.